



APPLICATIONS OF DUAL - ENERGY CT IN DISEASES OF THE URINARY SYSTEM

An Essay

Submitted for partial fulfillment of Master Degree in
Radiodiagnosis

By

Shrouk Mohamed Awadallah Bayomi

M.B.,B.CH.,

Faculty of Medicine – Ain Shams University

Supervised by

Prof. Dr. Annie Mohamed Nasr ElDin

Professor of Radiodiagnosis

Faculty of Medicine – Ain Shams University

Dr. Heba Ibrahimn

Lecturer of Radiodiagnosis

Faculty of Medicine – Ain Shams University

Faculty of Medicine
Ain Shams University



First and foremost, I thank Allah, the most beneficent and merciful.

*I am so grateful and most appreciative to the efforts of **Prof. Dr. Annie Mohamed Nasr ElDin**, Professor of Radio-diagnosis, Faculty of Medicine, Ain shams University, for her kind supervision, constructive guidance, continuous encouragement and valuable advices she offered me to achieve this work.*

*I wish to express my gratitude to **Dr. Heba Ibrahim**, Lecturer of Radio-diagnosis, Faculty of Medicine, Ain shams University for her kind assistance and guidance throughout the course of this essay.*

I am indebted to my family, my friends and my colleagues for their endless and continuous help and support.

Shrouk Mohamed



وَقُلْ اَعْمَلُوا فِى سَبِيلِ اللّٰهِ
عَمَلَكُمْ وَرَسُولُهُ وَالْمُؤْمِنُونَ



LIST OF CONTENTS

	Page
List of Abbreviations	ii
List of Figures	iii
List of Tables	v
Introduction and Aim of the Work.....	
Chapter ١:	
Anatomy of the urinary system.....	٤
Chapter ٢:	
Pathology of urinary lithiasis	٢٥
Chapter ٣:	
Physical aspects of dual energy multi detector computed tomography	٣٣
Chapter ٤:	
Role of dual energy multi detector CT in urinary diseases	٤٣
Summary and Conclusion.....	٨٧
References.....	٨٩
Arabic summary	-

LIST OF ABBREVIATIONS

<u>Abbreviation</u>	<u>Name</u>
CM	Contrast Material
CT	Computed Tomography
DE	Dual Energy
ESWL	Extracorporeal Shock Wave Lithotripsy
Fig.	Figure
FOV	Field of View
HIV	Human Immunodeficiency Virus
HU	Hounsfield Units
IV	Intra Venous
keV	Kilo Electron Volt
KUB =	Kidney, Ureter, Bladder
kV	Kilo Voltage
kVp	Peak Kilo Voltage
mAs	Milli Ampere
MDCT	Multi Detector Computed Tomography
MIP	Maximum Intensity Projection
MPR	Multi Planar Reconstruction
PCNL	Percutaneous Nephrolithotomy
SWL	Shock Wave Lithotripsy
UA	Uric Acid
VC	Virtual Contrast
VNC	Virtual Non Contract

LIST OF FIGURES

Fig. no.	Title	Page no.
CHAPTER 1: ANATOMY OF THE URINARY SYSTEM		
1,1	Retroperitoneal position of the kidneys in the posterior abdominal region.....	5
1,2	Internal structure of the kidney	6
1,3	Renal coverings	7
1,4	Organization of fat and fascia surrounding the kidney	9
1,5	Relations of the kidney.....	11
1,6	Posterior relations of the kidney.....	11
1,7	Renal vasculature	12
1,8	Drawing illustrates the normal anatomy of the renal arteries	13
1,9	Drawing illustrates the normal anatomy of the renal veins.....	14
1,10	Volume rendering reconstruction CT showing Sites of anatomical ureteric strictures	16
1,11	A sagittal section of the male and female pelvis.....	19
1,12	CT showing The two kidneys.....	21
1,13	Sagittal views (a and b) along the major axis of the kidneys more clearly evidence its anatomical relationships	22
1,14	CT showing Renal vasculature.....	23
1,15	CT showing both ureters	24
CHAPTER 2: PATHOLOGY OF URINARY LITHIASIS		
2,1	Chart illustrates commonly occurring urinary tract stones and describes their salient features.....	31
2,2	Flow chart depicts treatment decisions based on stone composition	32

Fig. no.	Title	Page no.
CHAPTER 3: PHYSICAL ASPECTS OF DUAL ENERGY MULTI DETECTOR COMPUTED TOMOGRAPHY		
3.1	Graph of mass-attenuation coefficients for iodine, calcium, and water on CT images obtained at two different energies	34
3.2	Dual-source CT system with a schematic illustration of the acquisition principle using 2 tubes and 2 corresponding detectors offset by 90 degrees	36
CHAPTER 4: ROLE OF DUAL ENERGY MULTI DETECTOR CT IN URINARY DISEASES		
4.1	Unenhanced CT scan shows normal renal parenchyma and the calculus in the inter polar portion of the right kidney	44
4.2	Contrast-enhanced CT scans obtained during the homogeneous nephrographic (A) and pyelographic phases (B) show the normal nephrographic progression	47
4.3	A, Transverse unenhanced dual-energy (combined 80/140 kVp) image shows left renal stone. B, Axial, color-coded overlay shows calcium-containing stone	53
4.4	Calcium oxalate stones	54
4.5	Uric acid stones	55
4.6	Dual-energy axial CT images show a left renal calculus with attenuation of 820 HU at 140 kVp (a) and 120 HU at 80 kVp (b). The calculus was determined to be composed of calcium oxalate monohydrate with the use of postprocessing techniques (c)	56
4.7	Color coded axial dual energy CT image showing a calcified calculus	56
4.8	Color coding based on the dual energy index of a stone shows that it consists of pure uric acid, and therefore is coded in red color	57
4.9	Dual-energy CT for stone characterization in two different patients. A, renal calculus color-coded blue, indicating non-uric acid stone. B, renal calculi color-coded red, indicating uric acid stone	58

Fig. no.	Title	Page no.
٤.١٠	Calcium-based stone, the calculus is shown in blue indicating a calcium-based stone.....	٥٩
٤.١١	Uric acid stone, the calculus is shown in red, indicating a uric acid stone.....	٥٩
٤.١٢	stone-targeted dual energy CT acquisition show stone in right ureter in which calcium salt component is represented in blue	٦١
٤.١٣	Transverse virtual unenhanced CT image reconstructed from contrast-enhanced dual-energy CT demonstrates urinary stone.....	٦٥
٤.١٤	Transverse virtual unenhanced CT reconstructed from contrast-enhanced dual-energy CT demonstrates right pelvic urinary stone	٦٦
٤.١٥	Transverse virtual unenhanced CT reconstructed from contrast enhanced dual-energy CT depicts right sided pelvicaliceal urinary stone disease	٦٦
٤.١٦	virtual non enhanced images show stone in right kidney, but a ٢-mm stone is not identifiable owing to over subtraction of stone signal.....	٦٧
٤.١٧	(a) True nonenhanced scan (b) Pyelographic-phase (c) Virtual non enhanced image.....	٦٨
٤.١٨	(a) Coronal excretory-phase image from dual-energy CT urography. (b) Coronal (virtual unenhanced) image obtained from the same CT image dataset (c) Axial unenhanced conventional CT image obtained in the same patient (d) Axial (virtual unenhanced) image from dual-energy CT, obtained at approximately the same level	٦٩
٤.١٩	Hyperattenuating renal cyst.....	٧٣
٤.٢٠	Renal cell carcinoma	٧٣
٤.٢١	Renal cell carcinoma	٧٤

LIST OF TABLES

Table no.	Title	Page no.
۱	Relative Advantages and Disadvantages of Different Dual-Energy CT Systems.....	۳۹

INTRODUCTION

Changes are occurring in medical CT that promises to augment the already well-recognized CT strengths of speed, high resolution, excellent patient tolerance, and large territory coverage. These changes include dose reduction, noise reduction, and more speed. But perhaps more fundamentally, the ability to perform dual-energy scanning at CT is being developed by every major CT scanner manufacturer and provides the ability for CT to differentiate between different materials at imaging. Dual-energy CT improves our ability to detect contrast material and distinguish the high-density areas created by iodine from those created by calcium or other substances—in essence, dual-energy CT brings the insight of tissue and material decomposition to standard gray-scale CT images (*Yeh et al*, ٢٠٠٩).

Dual-energy CT provides information about how substances behave at different energies, the ability to generate virtual unenhanced datasets, and improved detection of iodine-containing substances on low-energy images.

Knowing how a substance behaves at two different energies can provide information about tissue composition beyond that obtainable with single-energy techniques (*Coursey et al*, ٢٠١٠).

Several promising clinical applications for dual-energy computed tomography (CT) in genitourinary imaging have been reported. Dual-energy CT not only provides excellent morphologic detail but also can supply material-specific and quantitative information that may be particularly useful in

genitourinary imaging. Dual-energy CT has unique capabilities for characterizing renal lesions by quantifying iodine content and helping identify the mineral contents of renal stones, information that is important for patient care and therapeutic decision making (*Kaza et al*, ٢٠١٢).

Since the early ١٩٩٠s, the use of unenhanced CT has gained widespread acceptance in the evaluation of nephrolithiasis. Because studies have shown that helical CT can depict urinary stones more precisely than do radiography , sonography , nephrotomography , and excretory urography , MDCT has become the technique most used for rapid and accurate determination of the presence of stones in evaluations for urinary lithiasis treatment.

Precise determination of the symptoms, localization, size, and chemical composition of stones is the key to diagnosis and choice of therapy (*Grosjean et al*, ٢٠٠٨).

Dual Energy multidetector CT with advanced postprocessing techniques improves characterization of renal stone composition beyond that achieved with single-energy multidetector CT acquisitions with basic attenuation assessment (*Boll et al*, ٢٠٠٩).

So dual-energy CT will play an expanded role in the evaluation of patients with genitourinary disease in the future by providing expanded diagnostic information from CT images. Material characterization and diagnostic accuracy will be improved using dual energy CT (*Vrtiska et al*, ٢٠١٠).

AIM OF THE WORK

The aim of this work is to illustrate the role of dual energy multidetector CT in assessment of urinary diseases, mainly urinary stones.

CHAPTER 1

ANATOMY OF THE URINARY SYSTEM

THE KIDNEYS:

The bean-shaped kidneys are retroperitoneal in the posterior abdominal region. They lie in the extra peritoneal connective tissue immediately lateral to the vertebral column. In the supine position, the kidneys extend from approximately vertebra T¹¹ superiorly to vertebra L³ inferiorly, with the right kidney somewhat lower than the left because of its relationship with the liver. Although they are similar in size and shape, the left kidney is a longer and more slender organ than the right kidney, and nearer to the midline (fig. 1) (*Drake et al.*, 2012).

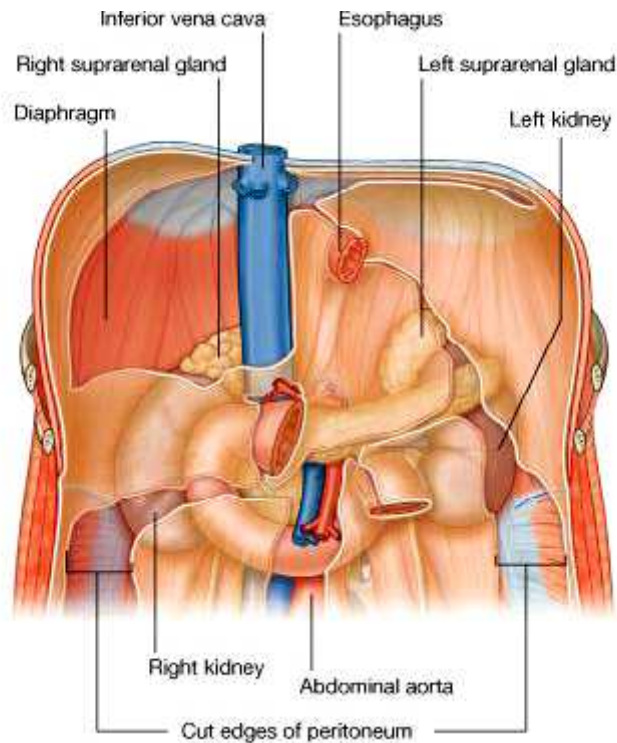


Figure 1.1: *Retroperitoneal position of the kidneys in the posterior abdominal region (quoted from Drake et al., 2012).*

The renal parenchyma is divided into outer lighter cortex and inner darker medulla (fig. 1.2). The medulla is composed of multiple, distinct, conically shaped areas termed renal pyramids, the apices of which are called renal papillae. Each papilla is cupped by an individual minor calyx. The sharp edged portion of each minor calyx extending around the papilla is called the calyceal fornix.

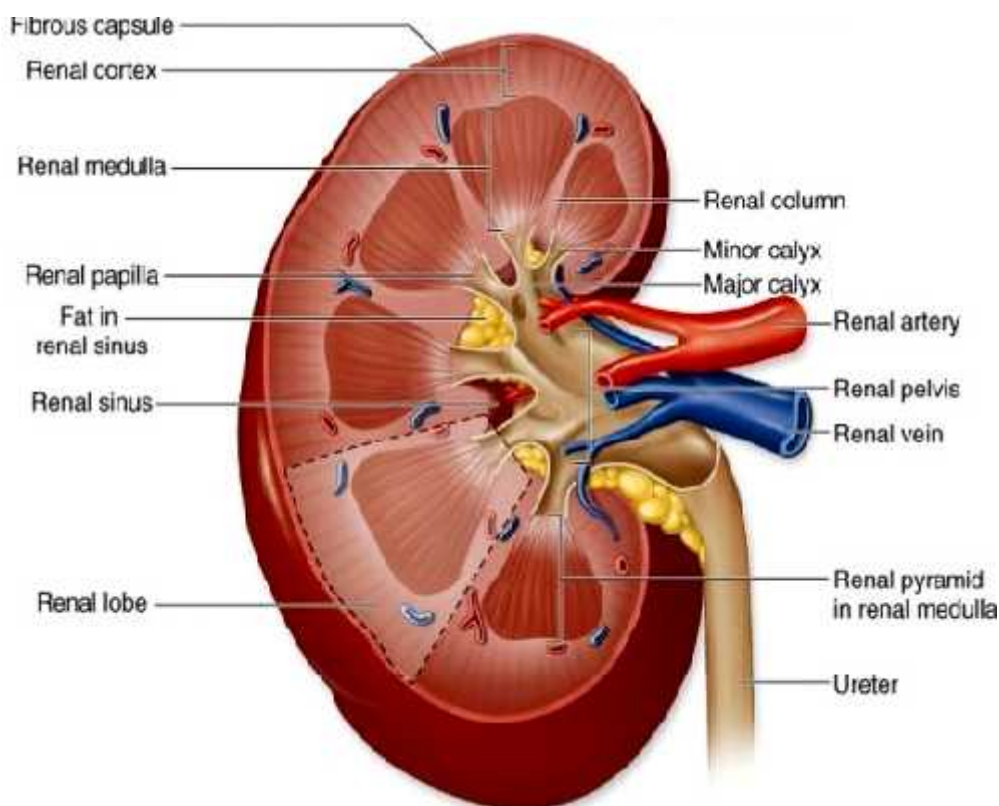


Figure 1.2: Internal structure of the kidney (quoted From Yaqoob, 2009).

The renal cortex is 1.2 to 1.5 cm in thickness, and not only covers the renal pyramids peripherally but also extends between the pyramids themselves forming the columns of Bertin. Through these columns renal vessels traverse from the renal sinus to peripheral cortex. So percutaneous access to the collecting system is made through a renal pyramid thus avoiding the columns of Bertin (Anderson et al., 2007).

On the medial margin of each kidney is the hilum which is a deep vertical slit through which renal vessels, lymphatics, and nerves enter and leave the substance of the kidney. Internally, the hilum is continuous with the renal sinus. Perinephric fat continues into the hilum and sinus and surrounds all structures (Drake et al., 2007).